Article:
Kern, Ralph, Zidarova, Radostina, Pietralla, Norbert et al. (35 more authors) (2020) Coulomb Excitation of Proton-rich N = 80 Isotones at HIE-ISOLDE. Journal of Physics: Conference Series. 012027. ISSN 1742-6596

https://doi.org/10.1088/1742-6596/1555/1/012027

Coulomb Excitation of Proton-rich $N = 80$ Isotones at HIE-ISOLDE

Journal of Physics: Conference Series **1555** (2020) 012027 doi:10.1088/1742-6596/1555/1/012027

Coulomb Excitation of Proton-rich $N = 80$ Isotones at HIE-ISOLDE

Ralph Kern[1], Radostina Zidarova[1], Norbert Pietralla[1], Georgi Rainovski[2], Liam P. Gaffney[3], Andrey Blazhev[4], Amar Boukhari[3], Joakim Cederkäll[3,5], James G. Cubiss[6], Martin Djongolov[2], Christoph Fransen[4], Kalin Gladnishki[2], Efstathios Giannopoulos[3,7], Herbert Hess[4], Jan Jolie[4], Vasil Karayonchev[4], Levent Kaya[4], James M. Keatings[8], Diana Kocheva[2], Thorsten Kröll[1], Oliver Möller[1], George G. O'Neill[9,10], Janne Pakarinen[7], Peter Reiter[4], Dawid Rosiak[4], Marcus Scheck[8], Jacob Snall[5], Pär-Anders Söderström[11], Pietro Spagnoletti[8], Robert Stegmann[1], Milena Stoyanova[2], Stefan Thiel[4], Andreas Vogt[4], Nigel Warr[4], Andree Welker[3], Volker Werner[1], Johannes Wiederhold[1], Hilde De Witte[12]

[1]Institut für Kernphysik, Technische Universität Darmstadt, Darmstadt, Germany
[2]Faculty of Physics, St. Kliment Ohridski University of Sofia, Sofia, Bulgaria
[3]CERN, Geneva, Switzerland
[4]Institut für Kernphysik, Universität zu Köln, Cologne, Germany
[5]Department of Nuclear Physics, University of Lund, Lund, Sweden
[6]Department of Physics, University of York, York, United Kingdom
[7]Department of Physics, University of Jyväskylä, Jyväskylä, Finland
[8]CEPS, University of the West of Scotland, Paisley, United Kingdom
[9]Department of Physics, University of Western Cape, Bellville, South Africa
[10]iThemba LABS, National Research Foundation, Somerset West, South Africa
[11]ELI-NP, Magurele, Romania
[12]Instituut voor Kern- en Strahlingsfysica, K.U. Leuven, Leuven, Belgium

E-mail: rkern@ikp.tu-darmstadt.de

Abstract. A projectile Coulomb-excitation experiment was performed at the radioactive ion beam facility HIE-ISOLDE at CERN. The radioactive ^{140}Nd and ^{142}Sm ions were post accelerated to the energy of 4.62 MeV/A and impinged on a 1.45 mg/cm^2-thin ^{208}Pb target. The γ rays depopulating the Coulomb-excited states were recorded by the HPGe-array MINIBALL. The scattered charged particles were detected by a double-sided silicon strip detector in forward direction. Experimental γ-ray intensities were used for the determination of electromagnetic transition matrix elements. Preliminary results for the reduced transition strength of the $\mathrm{B}(M1; 2_3^+ \rightarrow 2_1^+) = 0.35(19)\,\mu_\mathrm{N}^2$ of ^{140}Nd and a first estimation for ^{142}Sm have been deduced using the Coulomb-excitation calculation software GOSIA. The 2_3^+ states of ^{140}Nd and ^{142}Sm show indications of being the main fragment of the proton-neutron mixed-symmetry $2_{1,\mathrm{ms}}^+$ state.

1. Introduction

The origin of quadrupole collectivity in most heavy open-shell nuclei is the attractive quadrupole-quadrupole interaction between valence protons and neutrons. This interaction results in a coherent mixing of collective quadrupole excitations of the proton and neutron subspaces and leads to low-energy nuclear states, in which protons and neutrons collectively move in phase. Geometrical models are widely used to describe this collective motion. The nucleus is considered as a homogeneous object with a certain shape, which can vibrate or rotate [1]. However, this approach neglects the many-body character of the nuclear system.

A theoretical approach to the modeling of quadrupole-collective heavy nuclei, which provides a bridge to the calculation of nuclear properties from fundamental nucleon-nucleon interactions to the collective model, is the interacting boson model (IBM) [2]. The basic principle of the IBM is the coupling of nucleon pairs to bosons and treating both kinds of these bosons the same. The class of excited states emerging from the IBM describes the lowest-lying excitations in even-even nuclei, which are called full-symmetry states (FSSs). The IBM-2 [3], which additionally distinguishes between proton and neutron bosons, predicts another class of states, the mixed-symmetry states (MSSs). The proton and neutron motions of these states are partly out of phase.

To quantify the degree of coherence of the proton-boson and neutron-boson contribution, the F spin is introduced. The F spin is the analog of the isospin for nucleons for bosons. FSSs have the maximal F spin $F = F_{\max} = (N_\pi + N_\nu)/2$, where N_π and N_ν are the numbers of valence-proton and neutron bosons, respectively. However, MSSs are characterized by a lower F spin than the maximum: $F \leq F_{\max} - 1$. MSSs respresent a rare physics case in which the balance and interplay between nuclear collectivity, shell structure, and isospin degrees of freedom can be studied simultaneously. Furthermore, the only access to the quality of the F spin as a good quantum number is the determination of the mixing between FSSs and MSSs.

According to the IBM-2, the lowest-lying MSS in vibrational nuclei is the $2^+_{1,\mathrm{ms}}$ state. The most indicative experimental signature of the $2^+_{1,\mathrm{ms}}$ state is a strong $M1$ transition to the 2^+_1 state.

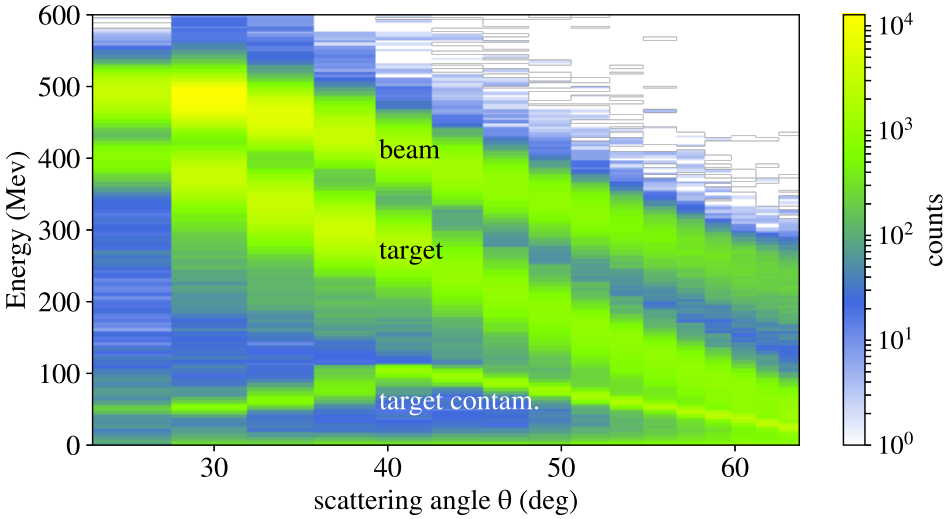

Figure 1. The spectrum of the DSSD shows the particle energy of the ^{208}Pb(^{140}Nd,^{140}Nd*)^{208}Pb reaction as a function of the scattering angle. Three different types of particles, heavy target, light target (contamination) and beam particles, are clearly separated.

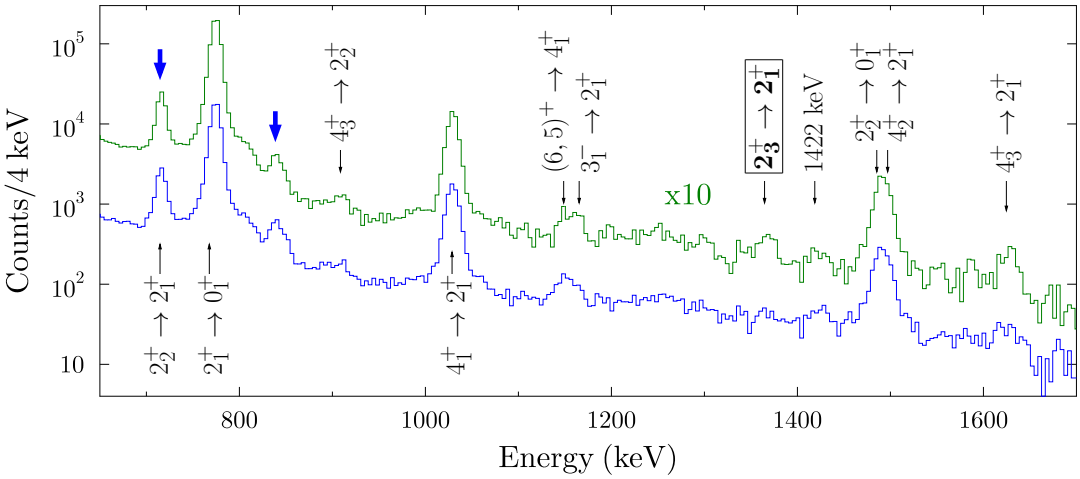

Figure 2. The time-random background subtracted, Doppler-corrected beam (green, scaled up by a factor of 10 for visibility) and target (blue) gated γ-ray singles spectra of the ^{208}Pb(^{140}Nd,^{140}Nd*)^{208}Pb reaction. The blue arrows mark transitions originating from the beam contaminant ^{140}Sm. The $2_3^+ \to 2_1^+$ transition is the most promising candidate for the strong $M1$ transition.

In contrast to isoscalar transitions between two FSSs with $\Delta F = 0$, isovector $M1$ transitions between MSSs and FSSs, with $\Delta F = 1$, are not suppressed. Available information on MSSs in the mass regions $A \approx 90, 130$ of vibrational nuclei has been summarized in a review article [4] and was recently extended for the mass $A \approx 200$ region [5, 6, 7]. The multipole-mixing ratio $\delta(2_i^+ \to 2_1^+)$ as well as the measurement of the absolute $M1$ transition strengths are indispensable for an unambiguous identification of MSSs.

The study of MSSs of the $N = 80$ isotonic chain reveals an interesting physics case. The nuclei ^{132}Te, ^{134}Xe and ^{136}Ba [8, 9, 10] form isolated $2^+_{1,\mathrm{ms}}$ states. In contrast, ^{138}Ce's $2^+_{1,\mathrm{ms}}$ state strongly mixes with a nearby full-symmetry 2^+ state [11]. This dramatic change in the properties of MSSs, when only two protons are added to the system, suggests that the strength concentration of collective isovector valence-shell excitations reflects the underlying single-particle structure through a mechanism dubbed shell stabilization [11]. The observed mixing in ^{138}Ce is attributed to the lack of shell stabilization at the $\pi g_{7/2}$ sub-shell closure. These experimental data lead to the expectation, that a direct experimental confirmation of the mechanism of shell stabilization in the $N = 80$ isotones should be sought for by identifying the MSSs in radioactive ^{140}Nd and ^{142}Sm.

2. Experiment

To study the evolution of MSSs in the proton-rich even-even $N = 80$ isotones, ^{140}Nd and ^{142}Sm, a projectile Coulomb-excitation (Coulex) experiment was performed at the radioactive ion beam (RIB) facility HIE-ISOLDE at CERN. A primary thick tantalum target was impinged by 1.4 GeV protons from the PS Booster. The panoply of isotopes produced via fusion, fragmentation and spallation were ionized by a combination of the hot surface ion source and the Resonance Ionization Laser Ion Source (RILIS) [12]. RILIS can selectively ionize the element of interest by applying an element specific multi-step resonance laser ionization scheme. The mass separation was done with the GPS dipole magnet followed by a post acceleration through REX and HIE cavities up to 4.62 MeV/A leading to an ion velocity of ≈ 9 % of the speed of light. During the

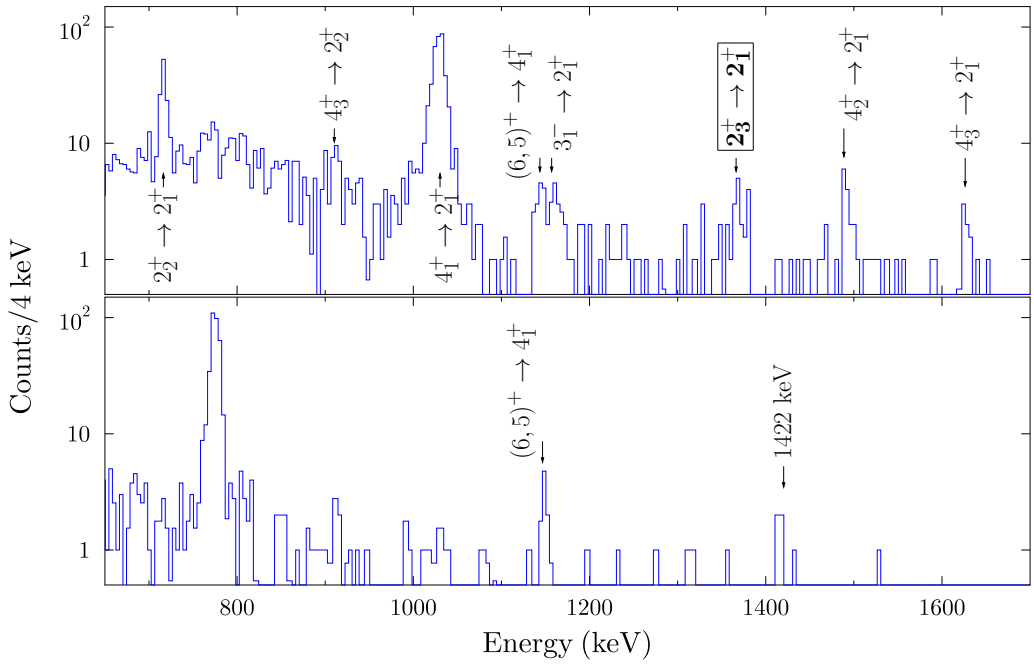

Figure 3. The time-random background subtracted, Doppler-corrected beam-particle gated γ-ray spectrum with the γ-ray coincidence condition on the $2_1^+ \rightarrow 0_1^+$ (top) and the $4_1^+ \rightarrow 2_1^+$ (bottom) transitions.

experiment, 5 - 10 x 10^5 particles per second were delivered to the MINIBALL experimental station. MINIBALL consists of 24 six-fold segmented high-purity germanium (HPGe) detectors which were focused on the secondary target, a 1.45 mg/cm^2-thin ^{208}Pb foil. The beam energy was chosen sufficiently low to ensure that for the detected scattered particles, the distance between the reaction partners is greater than 5 fm [13]. This is considered "safe" Coulex and, hence, nuclear reactions besides Coulex can be neglected. The scattered particles, beam and target, are detected by a double-sided silicon strip detector (DSSD) placed in the forward direction, covering 23° - 63° in the laboratory frame with respect to the beam axis. The γ rays depopulating the Coulomb-excited states were detected by MINIBALL. The total periods of measurement were one day and five days for the ^{140}Nd and the ^{142}Sm ion beams, respectively.

With the particle-energy spectrum of the DSSD (cf. Figure 1), three different kinds of particles can be identified: the two broad bands – high and low energy – are the beam, ^{140}Nd, particles and the heavy target, ^{208}Pb, particles, respectively, whereby the narrow band at very low energies belongs to target-like particles from a small amount of oxygen contamination of the target. The known kinematics of the scattering process allows one to distinguish between target- and beam-particle hits on the DSSD. The information about the velocity and the type of the scattered particle is used to correct the γ-ray energies for the Doppler shift. The $A = 140$ beam consists of approximately 2/3 ^{140}Nd and 1/3 ^{140}Sm, when comparing the γ-ray intensities of the $2_1^+ \rightarrow 0_1^+$ transitions. For the $A = 142$ beam, no γ-rays originating from a different isotope than ^{142}Sm were observed.

3. Data Analysis

The connection between the relative cross sections and the relative population yields of Coulomb-excited states is used in the "safe" Coulex method in order to determine reduced transition strengths. Hence, a quantity is needed to normalize on. For this purpose recently analog Coulex

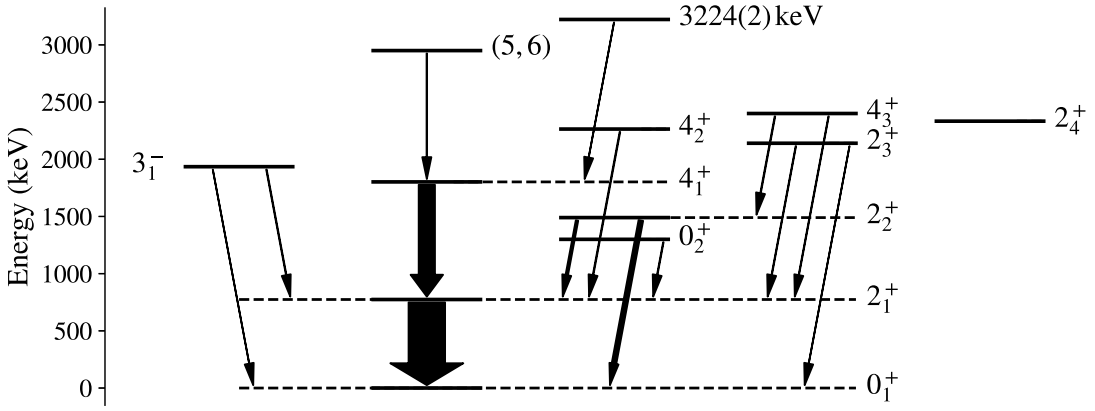

Figure 4. The partial level scheme of ^{140}Nd. The widths of the transitions correspond to the observed intensities. The $2_1^+ \rightarrow 0_1^+$ transition width is scaled down by a factor of 5 for visibility.

experiments at REX-ISOLDE have been performed to determine the reduced transition strength $\mathrm{B}(E2; 2_1^+ \rightarrow 0_1^+)$ relative to the target excitation [14, 15]. The $\mathrm{B}(E2; 2_1^+ \rightarrow 0_1^+)$ values at 33(2) W.u. and 32(4) W.u. for ^{140}Nd and ^{142}Sm, respectively, have been used for the normalization for this experiments and no target-excitation normalization was needed.

The relative populations of states have been deduced by intensities of the depopulating γ rays taking the relative efficiency, known branching ratios and the theoretical electron conversion coefficients [16] into account. Particle-γ-γ coincidences were used to resolve doublets of transitions, which were inseparable in the particle-γ spectra (cf. Figures 2 and 3). The obtained information from the singles and coincidence spectra has been used to produce a partial level scheme of ^{140}Nd including the observed transitions (cf. Figure 4).

Finally, the Coulex calculation code GOSIA [17] has been used to fit transition matrix elements (MEs) to the experimental population yields. The Coulex calculations are solely sensitive to the excitation, not to the de-excitation process. Therefore, regarding the state of interest, $2_{1,\mathrm{ms}}^+$, primarily the ME $\langle 2_{1,\mathrm{ms}}^+ || E2 || 0_1^+ \rangle$ can be determined, because it is its main excitation path. The reduced transition strength of interest, $\mathrm{B}(M1; 2_{1,\mathrm{ms}}^+ \rightarrow 2_1^+)$, can be obtained by adding spectroscopic information, such as the branching ratio of the $2_{1,\mathrm{ms}}^+$ state and the multipole mixing ratio of the $2_{1,\mathrm{ms}}^+ \rightarrow 2_1^+$ transition, to the GOSIA calculations.

Many different experiments were performed to date, trying to identify the MSS of ^{140}Nd, e.g. a β-decay [18] and a Doppler-shift attenuation method experiment [19]. Both experiments concluded that the 2_3^+ state was the most promising candidate for the $2_{1,\mathrm{ms}}^+$ state. However, in order to identify the main fragment of the MSS it is important to determine the reduced $M1$ transition strength of the $2_3^+ \rightarrow 2_1^+$ transition. The preliminary result of GOSIA calculations using a small subset of states is a reduced $M1$ transition strength of $\mathrm{B}(M1; 2_3^+ \rightarrow 2_1^+) = 0.34(19)\,\mu_\mathrm{N}^2$. The detection limit of three σ leads to an upper limit for the reduced $M1$ transition strength of $\mathrm{B}(M1; 2_4^+ \rightarrow 2_1^+) < 0.035(20)\,\mu_\mathrm{N}^2$. Hence, the preliminary results clearly favor the 2_3^+ state as the main fragment of the $2_{1,\mathrm{ms}}^+$ state and the 2_4^+ state as a small fragment.

The situation for ^{142}Sm is different. Presently, there is no available information on the multipole-mixing ratios of $2_\mathrm{i}^+ \rightarrow 2_1^+$ transitions. There are clear similarities in the level structures of ^{140}Nd and ^{142}Sm (cf. Figure 5). Hence, as a first approximation one may assume the $2_3^+ \rightarrow 2_1^+$ transition of ^{142}Sm as a pure $M1$, as in ^{140}Nd, for a rough estimation. The $2_3^+ \rightarrow 2_1^+$ transition of ^{142}Sm is also present in the particle-γ spectra of the ^{208}Pb(^{142}Sm,^{142}Sm*)^{208}Pb reaction. Preliminary results from GOSIA calculations show a reduced transition strength of

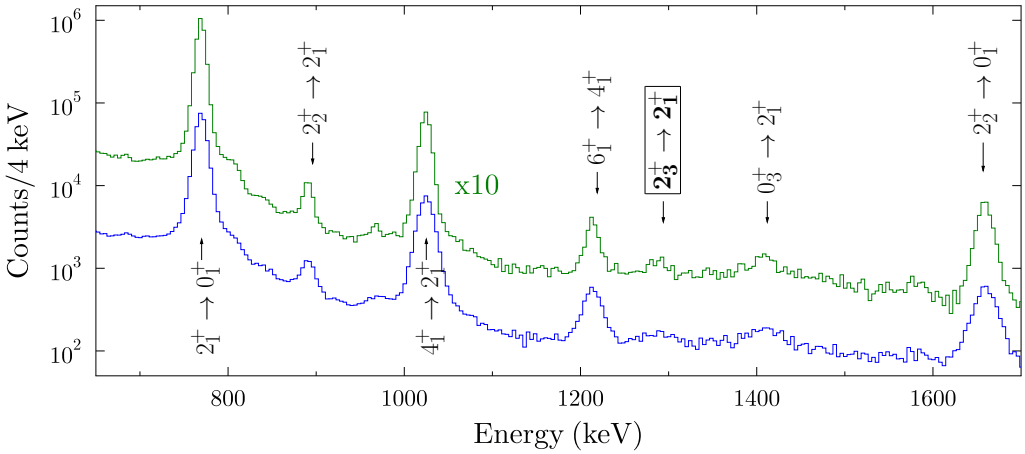

Figure 5. The time-background subtracted, Doppler-corrected beam (green, scaled up by a factor of 10 for visibility) and target (blue) gated γ-ray singles spectra of the ^{208}Pb(^{142}Sm,^{142}Sm*)^{208}Pb reaction.

$B(M1; 2_3^+ \to 2_1^+) \approx 0.3\,\mu_N^2$, which further supports assigning the 2_3^+ state of ^{142}Sm as the $2_{1,ms}^+$ state.

4. Discussion

IBM-2 and QPM calculations for the stable $N = 80$ isotones ^{134}Xe, ^{136}Ba and ^{138}Ce reproduce the experimental $B(M1, 2_i^+ \to 2_1^+)$ distributions for these nuclei with high accuracy [20]. These calculations also predict the decrease of the energy of the $2_{1,ms}^+$ state, when additional protons start to fill the shell beyond the $\pi g_{7/2}$ sub-shell closure. This prediction is supported by the preliminary results, for ^{140}Nd as well as for ^{142}Sm. The $N = 84$ isotonic chain, which is the valence-neutron particle conjugate to the $N = 80$ chain, reveals a strong splitting of the $B(M1, 2_i^+ \to 2_1^+)$ strength for ^{142}Ce and ^{144}Nd [21, 22, 23]. Such a strong splitting could not be observed for ^{140}Nd, which may indicate the strong effect of sub-shell structures and of the specific orbitals, that are involved in the valence shell, on low-lying collective excitations.

Finally, a simple two-state mixing scenario is introduced to determine the mixing of the F spin of ^{140}Nd. The F-spin mixing matrix element V_{mix} is the indicator of the actual strength of the mixing between FSSs and MSSs. The 2_3^+ and the 2_4^+ states are superpositions of the theoretical fully-symmetric 2_{FSS}^+ and the mixed-symmetric 2_{MSS}^+ states. In this case, the whole $M1$ strength is focused on the isovector ($\Delta F = 1$) $2_{MSS}^+ \to 2_1^+$ transition, whereby the $M1$ transition between two FSSs ($\Delta F = 0$) is highly suppressed. The simultaneous determination of the $B(M1; 2_3^+ \to 2_1^+)$ and the upper limit of the $B(M1; 2_4^+ \to 2_1^+)$ strengths enables the calculation of a preliminary upper limit of $V_{mix} < 55(17)$ keV. A reduction of V_{mix} from ^{138}Ce ($V_{mix} = 44(3)^{+3}_{-14}$ keV) to ^{140}Nd was excluded by a previous multipole-mixing ratio measurement [18] ($V_{mix} = 92(14)$ keV). This preliminary upper limit for the F-spin mixing indicates a lower value as reported in Ref. [18] and a reduction of V_{mix} is conceivable (cf. Figure 6).

5. Summary

For ^{140}Nd, a preliminary result and an upper limit of the reduced M1 transition strength of the $2_3^+ \to 2_1^+$ and $2_4^+ \to 2_1^+$ transitions have been determined via GOSIA calculations, respectively. Consequently, a preliminary upper limit for the F-spin mixing matrix element has also been deduced $V_{mix} < 55(17)$ keV. In ^{142}Sm, first calculations indicate the 2_3^+ state as the main

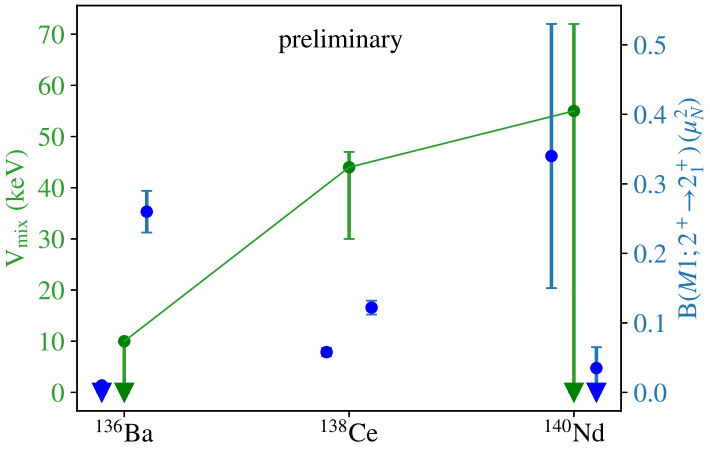

Figure 6. The $M1$ transition strengths $B(M1; 2_i^+ \rightarrow 2_1^+)$ of the fragments of the $2_{1,ms}^+$ state of $N = 80$ isotones are shown in blue. The resulting F-spin mixing matrix elements are shown in green.

fragment of the MSS using the assumption of a pure $M1$ character of the $2_3^+ \rightarrow 2_1^+$ transition as in ^{140}Nd. The preliminary results indicate a focused $M1$ strength in one fragment of the MSS in both radioactive $N = 80$ isotones ^{140}Nd and ^{142}Sm. The lack of fragmentation supports the hypothesis of the isovector valence-shell re-stabilization after the proton sub-shell closure of ^{138}Ce.

Acknowledgements
This work was supported by the BMBF grants Nos. 05P18RDCIA, 05P19RDFN1, 05P18RDFN9 and 05P18PKCIA, by the BgNSF grant DN08/23/2016, by grants from the U.K. Science and Technology Facilities Council, and the European Union within the Horizon 2020 research and innovation programme (ENSAR-2). The UWS group acknowledges financial support by the UK-STFC.

References
[1] A. Bohr and B. Mottelson, *Nuclear Structure* (Benjamin, Reading, MA, 1975), Vol. II.
[2] A. Arima et al., Phys. Lett. B **66**, 205 (1997).
[3] F. Iachello Phys. Rev. Lett. **53** 1427 (1984).
[4] N. Pietralla et al., Phys. Rev. C **64** 031301(2001).
[5] D. Kocheva et al., Phys. Rev. C **93**, 011303 (2016).
[6] R. Stegmann et al., Phys. Lett. B **770**, 77 (2017).
[7] R. Kern et al., Phys. Rev. C **99**, 011303(R) (2019).
[8] M. Danchev et al., Phys. Rev. C **84**, 61306, (2010).
[9] T. Ahn et al., Phys. Lett. B **679**, 19 (2009).
[10] N. Pietralla et al., Phys. Rev. C **58**, 796 (1998).
[11] G. Rainovski et al., Phys. Rev. Lett. **69**, 122501 (2006).
[12] V.N. Fedosseev et al., Nucl. Instr. and Methods in Phys. Res. B **266**, 4378 - 4382 (2008).
[13] D. Cline Ann. Rev. Nucl. Part. Sci. **36**, 683 (1986).
[14] C. Bauer et al., Phys. Rev. C **88**, 021302 (2013).
[15] R. Stegmann et al., Phys. Rev. C **91**, 054326 (2015).
[16] T. Kibédi et al., Nucl. Instr. and Methods in Phys. Res. Sec. A **589**, 202 (2008).
[17] T. Czosnyka et al., Bulletin of the American Physical Society **28**, 745 (1983).
[18] E. Williams et al., Phys. Rev. C **80**, 054309 (2009).
[19] K. Gladnishki et al., Phys. Rev. C **82**, 037302 (2010).

[20] N. Lo Iudice, Ch. Stoyanov, D. Tarpanov, Phys. Rev. C **77**, 044310 (2008).
[21] J. R. Vanhoy et al., Phys. Rev. C **52**, 2387 (1995).
[22] S. F. Hicks et al., Phys. Rev. C **57**, 2264 (1998).
[23] N. Lo Iudice et al., J. Phys. G: Nucl. Part. Phys. **39** 043101 (2012).